AIP | Applied Physics Letters

Efficient infrared electroabsorption with 1 V applied voltage swing using intersubband transitions

P. Holmström, P. Jänes, U. Ekenberg, and L. Thylén

Citation: Applied Physics Letters **93**, 191101 (2008); doi: 10.1063/1.3013360
View online: http://dx.doi.org/10.1063/1.3013360
View Table of Contents: http://scitation.aip.org/content/aip/journal/apl/93/19?ver=pdfcov
Published by the AIP Publishing

Efficient infrared electroabsorption with 1 V applied voltage swing using intersubband transitions

P. Holmström,[a] P. Jänes,[b] U. Ekenberg, and L. Thylén
Department of Microelectronics and Applied Physics, Royal Institute of Technology (KTH), SE-164 40 Kista, Sweden

(Received 3 June 2008; accepted 13 October 2008; published online 10 November 2008)

We have demonstrated efficient intersubband electroabsorption in InGaAs/InAlGaAs/InAlAs step quantum wells grown by metal-organic vapor-phase epitaxy. An absorption modulation of 6 dB ($\Delta\alpha$=2300 cm^{-1}) at $\lambda\sim5.7$ μm due to Stark shift of the intersubband resonance was achieved at a low applied voltage swing of ±0.5 V in a multipass waveguide structure. The interface intermixing was estimated by comparing experimental and theoretical Stark shifts. It is predicted that the present material in a strongly confining surface plasmon waveguide can yield an electroabsorption modulator with a peak-to-peak voltage of V_{pp}=0.9 V and modulation speed of $f_{3dB}\approx130$ GHz. © *2008 American Institute of Physics*. [DOI: 10.1063/1.3013360]

Intersubband (IS) transitions have primarily been applied to quantum-well infrared photodetectors (QWIPs) (Ref. 1) and quantum cascade lasers (QCLs).[2] However, the properties of IS transitions are also attractive for application to electroabsorption (EA) modulators. A fundamental advantage of IS transitions is that the electron subbands are essentially parallel to each other. The ensuing weak dependence of the transition energy on the in-plane wave vector results in sharply peaked IS resonances and a potential for strong absorption implying compact modulators. The broadening of the peaks due to subband nonparabolicity has been shown to be effectively cancelled by collective phenomena.[3] A small IS absorption linewidth Γ is imperative for a high *RC*-limited speed in IS-based EA modulators as generally the modulator capacitance $C\sim\Gamma^3$.[4] Other advantages are the rapid IS relaxation time of only ~1 ps, which enables saturation resistant modulators, and the possibility to achieve a negative chirp parameter.[5]

IS-based modulation has previously been demonstrated at mid-IR wavelengths;[6,7] however, it used rather large voltages of 5–10 V due to large numbers of QWs. In this letter we show experimentally that an absorption modulation of up to 6 dB at $\lambda\sim5.7$ μm due to Stark shift of the IS absorption can be achieved with a voltage swing as low as ±0.5 V. The QW interface intermixing is subsequently estimated by comparing experimental and theoretical Stark shifts. Finally, based on the experimental results we estimate that an EA modulator with a modulation speed as high as $f_{3dB}\approx130$ GHz can be realized with the present material by using a strongly confining surface plasmon waveguide. The structures examined here in many respects coincide with the one we previously evaluated in a modulator simulation.[4]

The samples were grown in an Aixtron AIX-200 MOVPE system on semi-insulating InP:Fe substrates. First a 500 nm *n*-InP (5×10^{17} cm^{-3}) buffer layer was grown. It was followed by a 60 nm lattice-matched *n*-AlGaInAs (x_{Al}=0.37, 5×10^{17} cm^{-3}) layer, which was grown immediately before the multiple-quantum-well (MQW) layer, with a similar one just after the MQW. The purpose of these two *n*-AlGaInAs layers is to line up the Fermi energies inside and outside the MQW without bend bending[4] in order to obtain the same IS transition energies in all step QWs. On top of the upper 60 nm *n*-AlGaInAs layer a 550 nm *n*-InP (5×10^{17} cm^{-3}) cap layer was grown. Each step QW consisted of a 3.8 nm InGaAs well layer and a 5.9 nm AlGaInAs step layer, separated by 17 nm InAlAs barrier layers. The barriers were Si δ-doped at $n_D=2.2\times10^{12}$ cm^{-2} to supply electrons in the step QWs. The δ-dopings were performed by halting the growth while supplying SiH_4, whereafter the growth proceeded without further delay. Each sample had an MQW comprising ten step QWs. Two samples 5789 and 5791 were grown, which differed by the position of the δ-doping layer. The potential profile of one step QW in 5789 without any applied bias voltage is shown in Fig. 1.

Structural characterization of the grown samples was performed by a combination of high-resolution x-ray diffraction (XRD) measurements and simulation of the two observed IS resonances $1\rightarrow2$ and $1\rightarrow3$. By XRD 2θ-ω scans the MQW period $L_p=26.7\pm0.2$ nm in the samples could be reliably obtained. However since the MQW comprises a

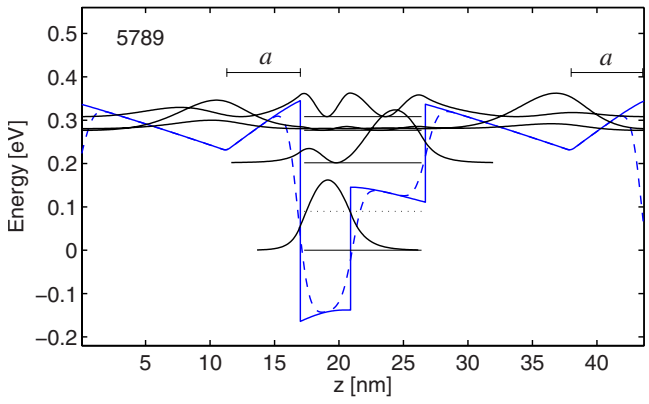

FIG. 1. (Color online) Potential profile of the step QW of 5789 with no applied bias voltage. Also shown are the moduli squared of the bound states in the step QW as well as two mostly barrier confined states. The dotted line indicates the Fermi energy. The samples 5789 and 5791 differ by the spacer layer thickness a=5.6 and 8.3 nm, respectively, between the δ-doping layer and the InGaAs QW layer. The dashed line represents the intermixed conduction band potential with the diffusion length L_d=5 Å.

[a]Electronic mail: petterh@kth.se.
[b]Present address: Proximion Fiber Systems AB, SE-164 40 Kista, Sweden.

repetition of three different and nearly lattice-matched layers, viz., the InGaAs well layer, the InAlGaAs step layer, and the InAlAs barrier; the individual thicknesses and compositions of these were not available from XRD results alone. However the IS peak energies $\tilde{E}_{12}$ and $\tilde{E}_{13}$ as well as the ratio between the two oscillator strengths f_{13}/f_{12} add enough information to determine the thickness of the well and step layers given above as well as the conduction band edge of the step layer corresponding to a composition of $Al_{0.31}Ga_{0.16}In_{0.53}As$.

The IS transition energies were modeled in the envelope function approximation considering the nonparabolicity of the conduction band.[8] Material parameters were obtained from the review paper by Vurgaftman *et al.*[9] As the sheet electron density is quite high in the step QWs, we solve for the step QW potential self-consistently including the Hartree space-charge potential and an exchange-correlation potential.[10,11] The exchange-correlation effects are thus included as a one-particle exchange-correlation potential. Further we also considered the collective shift of the IS resonance peak due to the depolarization and exciton effects.[12]

The room-temperature IS absorption spectra of the two samples without applied bias voltage are shown in Fig. 2(a). Both exhibit a full width at half maximum linewidth of the $1\rightarrow2$ transition of 26 meV despite some difference in the spacer layer thickness a. The IS absorption was characterized in a multipass geometry in the usual fashion where two beveled edges and the back side of a 5×7 mm^2 piece were polished to allow multiple internal reflections. The spectra were measured using Fourier-transform infrared (FT-IR) spectroscopy, and isolation of the IS absorbance was achieved by taking the ratio of the transmittance spectra of TM and TE-polarized light, $A=-\log_{10}(T_{TM}/T_{TE})$. In addition, a smooth background offset due to the polarization dependence in the FT-IR spectrometer was subtracted. Due to polarization selection rules IS transitions almost exclusively couple to TM-polarized light. No significant absorption was observed for TE-polarized light.

To enable voltage to be applied over the MQWs Ti/Pt/Au contacts were deposited on the n-InP cap layer and on the buffer n-InP layer below the MQW stack. The bottom contact was deposited after lithography and dry-etching down to the bottom contact layer. The contacts were performed as stripes 5×0.2 mm^2 with a distance of 4 mm between them. Clear Stark shifts of the $1\rightarrow2$ and $1\rightarrow3$ IS resonances were observed at low applied voltages (Fig. 2(b)). The EA was characterized while keeping the samples in a liquid-nitrogen cryostat at T=77 K, which was necessary due to the large area of the multipass device. The IS linewidth reduced only slightly to 25 meV at low temperature. Even at 77 K IV-characterization revealed some current through the device. The ensuing small voltage drop in the contact layers was modeled considering that the device resistance R is composed of two parts in series $R=R_{lat}+R_{MQW}$. The resistance R_{lat} is associated with the lateral conduction in the n-InP contact layers and laterally in the MQW. The voltage that is applied over the MQW is then obtained by voltage division, i.e., $V_{b,MQW}=V_b(R-R_{lat})/R$. The bias dependent multipass device resistance $R=V_b/I$, where I is the current through the device. At high bias, R asymptotically approaches R_{lat}, which is set to 25 Ω, in agreement with what can be calculated for the structure. At a bias voltage of $V_b=\pm0.5$ V, the device

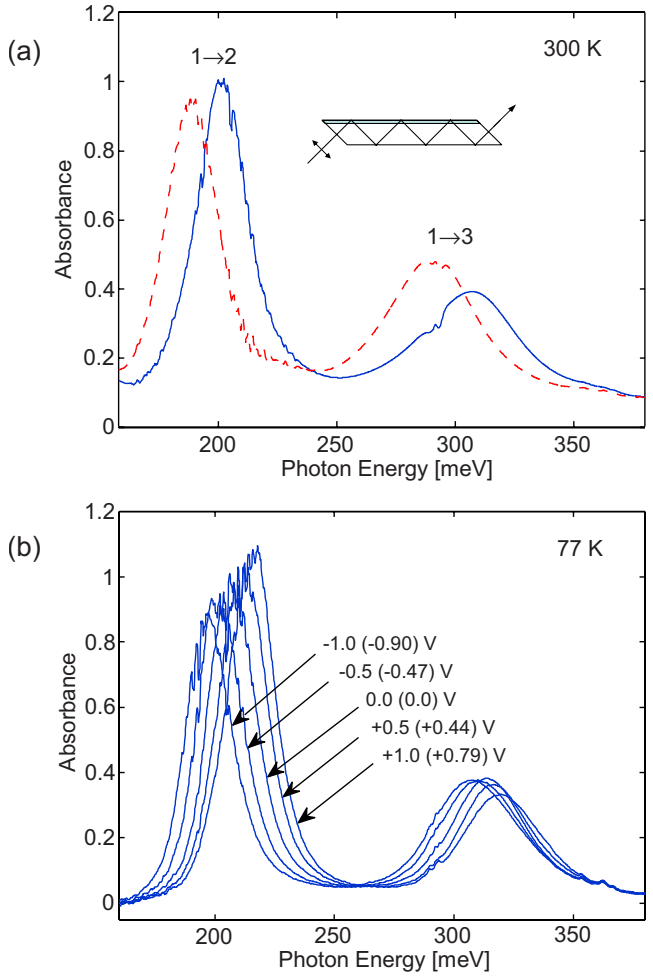

FIG. 2. (Color online) (a) Absorption spectra measured at room-temperature with no applied bias ($V_b=0$ V) for the samples 5789 (solid) and 5791 (dashed). Absorption peaks due to the $1\rightarrow2$ and $1\rightarrow3$ IS transitions are visible. Inset: schematic multipass characterization geometry. (b) Absorption spectra measured in 5789 for different applied voltages at T=77 K. Clear Stark shifts of the $1\rightarrow2$ and $1\rightarrow3$ IS resonances are observed. Indicated for each spectrum is the applied voltage V_b and within parentheses the voltage over the MQW $V_{b,MQW}$.

resistance is a few hundred ohms (current density $J\sim5$ mA/cm^2) so that the relative voltage drop over the MQW $V_{b,MQW}/V_b\approx0.9$, as indicated in Fig. 2(b). The magnitude of the current agrees well with tunneling in the MQW through the QW ground states, while thermionic emission is completely suppressed in this structure at 77 K. The device current can be efficiently reduced by decreasing the device dimensions, e.g., in waveguide modulators.

The shift of the $1\rightarrow2$ IS resonance due to the Stark effect in both samples is shown in Fig. 3. The difference in IS resonance energy between the samples, seen in both experimental and calculated values, is due to the doping position affecting the electric field over the step QW. In Fig. 3 the voltage drop in the contact layers was compensated for by plotting the IS absorption peak positions versus the voltage over the MQW, $V_{b,MQW}$. The experimental Stark shifts are still about 20% smaller than the calculated ones for sharp interfaces. The main reason for the discrepancy is likely the intermixing of the QW interfaces. By assuming intermixed interfaces with a diffusion length $L_d=5$ Å (1.7 monolayers), as shown in Fig. 1, we obtain good quantitative agreement with the experimental Stark shifts. IS based structures have

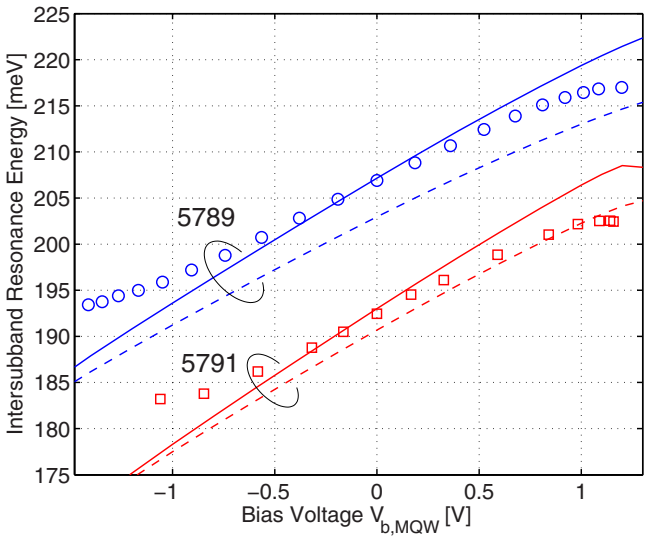

FIG. 3. (Color online) Stark shift of the $1\rightarrow 2$ IS absorption peak position vs the voltage $V_{b,\mathrm{MQW}}$ applied over the MQW. The symbols indicate experimental IS peak positions in the samples 5789 (circles) and 5791 (squares). The calculated $1\rightarrow 2$ IS resonance energies with sharp and intermixed (L_d=5 Å) interfaces are indicated by solid and dashed lines, respectively.

generally been grown by molecular-beam epitaxy owing to its better control of small layer thicknesses and lower growth temperatures, which should reduce interface intermixing. The present structures were, however, grown by MOVPE, which is considered more suitable for commercial production.

Following Ref. 4 we can predict the performance of high-speed modulators based on a surface-plasmon (SP) waveguide (Fig. 4). The SP is supported by the gold contact layer placed closely on top of the MQW. From the EA spectra in Fig. 2(b) we deduce an absorption change in $\Delta\alpha = 2300\ \mathrm{cm}^{-1}$ in the MQW for purely TM-polarized light with an applied voltage swing over the MQW of $V_{\mathrm{pp}}=0.9$ V.[13] Inserting this experimental MQW material in the simulated SP waveguide (Fig. 4), we obtain an active modulator length as short as 30 μm for a 10 dB extinction ratio. In simulations for sharp interfaces we have predicted very high *RC*-limited room-temperature modulation speeds $f_{3\mathrm{dB}}$ at low voltages,[4,14] e.g., $f_{3\mathrm{dB}}\approx 190$ GHz at a driving voltage of only $V_{\mathrm{pp}}=0.9$ V.[4] Based on the experimental results in this paper it should still be possible to reach $f_{3\mathrm{dB}}\approx 130$ GHz, assuming a modulator mesa width $w=2$ μm and a 50 Ω driver impedance.

High-speed IS modulators operating at $\lambda\sim 5.7$ μm can be useful for interconnects with Si waveguides, utilizing

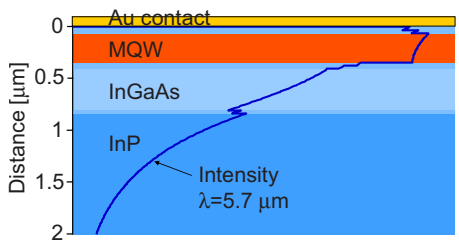

FIG. 4. (Color online) Layer structure and optical mode intensity profile of a SP-based modulator.

the Si transmission window of 1.2–6.5 μm.[15] The atmospheric absorption at the present wavelength is rather large. However with a slightly different step QW design, it should be no problem to reach the windows at $\lambda=3-5$ μm and $\lambda=8-14$ μm. Such modulators would be very valuable for free-space communication, an area of increasing importance.[16] In addition, the absorption due to fogs and dust is an order of magnitude or more lower than at the commonly used communication wavelengths of 850, 1300, and 1550 nm.[17] The present predicted speed is much higher than the *RC*-limited speeds of ~10 GHz hitherto achieved by direct modulation of QCLs.[18] As for light sources, continuous-wave operation of QCLs with high power at room temperature has been demonstrated in recent years.[19] The concept of IS modulators is also promising for fiber-optical communication wavelengths such as $\lambda=1.55$ μm. This implementation requires material pairs with very large conduction band offsets. Such materials are generally less mature resulting in clearly larger linewidths Γ, but with continued improvement in sample quality they should become superior to present interband modulators.[5]

In conclusion we have measured efficient EA in InP-based step QW structures. Sufficient Stark shifts were obtained with an applied voltage swing of 1.0 V. Intermixing with a diffusion length of L_d=5 Å was estimated in the QWs. The results indicate that a 30 μm long modulator with a surface plasmon waveguide can reach a speed exceeding $f_{3\mathrm{dB}}\sim 100$ GHz.

The authors are grateful to A. Patel for growing the samples by MOVPE. This work was supported by the Swedish Research Council (VR).

[1] H. Schneider and H. C. Liu, *Quantum Well Infrared Photodetectors: Physics and Applications* (Springer, Berlin, 2007).
[2] J. Faist, D. Hofstetter, M. Beck, T. Aellen, M. Rochat, and S. Blaser, Proc. SPIE **4651**, 274 (2002).
[3] R. J. Warburton, K. Weilhammer, C. Jabs, J. P. Kotthaus, M. Thomas, and H. Kroemer, Physica E (Amsterdam) **7**, 191 (2000).
[4] P. Holmström, IEEE J. Quantum Electron. **37**, 1273 (2001).
[5] P. Holmström, IEEE J. Quantum Electron. **42**, 810 (2006).
[6] R. P. G. Karunasiri, Y. J. Mii, and K. L. Wang, IEEE Electron Device Lett. **11**, 227 (1990).
[7] H. C. Liu, C. Y. Song, A. SpringThorpe, and G. C. Aers, Electron. Lett. **39**, 1149 (2003).
[8] C. Sirtori, F. Capasso, J. Faist, and S. Scandolo, Phys. Rev. B **50**, 8663 (1994).
[9] I. Vurgaftman, J. R. Meyer, and L. R. Ram-Mohan, J. Appl. Phys. **89**, 5815 (2001).
[10] L. Hedin and B. I. Lundqvist, J. Phys. C **4**, 2064 (1971).
[11] W. L. Bloss, J. Appl. Phys. **66**, 3639 (1989).
[12] T. Ando, Solid State Commun. **21**, 133 (1977).
[13] P. Holmström, P. Jänes, U. Ekenberg, and L. Thylén, J. Phys.: Conf. Ser. **100**, 042009 (2008).
[14] P. Jänes, P. Holmström, and U. Ekenberg, IEEE J. Quantum Electron. **38**, 178 (2002).
[15] B. Jalali and S. Fathpour, J. Lightwave Technol. **24**, 4600 (2006).
[16] For a review, see D. Killinger, Opt. Photonics News **13**, 36 (2002).
[17] R. Martini, C. Glazowski, E. A. Whittaker, W. W. Harper, Y.-F. Su, J. F. Shultz, C. Gmachl, F. Capasso, D. L. Sivco, and A. Y. Cho, Proc. SPIE **5359**, 196 (2004).
[18] R. Paiella, R. Martini, F. Capasso, C. Gmachl, H. Y. Hwang, J. N. Baillargeon, D. L. Sivco, A. Y. Cho, E. A. Whittaker, and H. C. Liu, Appl. Phys. Lett. **79**, 2526 (2001).
[19] J. Faist, Opt. Photonics News **17**, 32 (2006).